UNIVERSITÀ DEGLI STUDI DI PADOVA

DIPARTIMENTO DI BIOLOGIA

Corso di Laurea in Scienze Naturali

ELABORATO DI LAUREA

VOLCANOLOGICAL IMPLICATIONS INFERRED FROM CHEMICAL ANALYSES OF OLIVINES COLLECTED AT SÃO JORGE ISLAND (AZOREAN ARCHIPELAGO, PORTUGAL)

Tutor: Prof. Andrea Marzoli
Dipartimento Territorio e Sistemi Agro-Forestali (TESAF)

Co-tutor: Prof. Davide Novella
Dipartimento di Geoscienze

Laureanda: Erica Luce Beghini

ANNO ACCADEMICO 2022/2023

UNIVERSITÀ DEGLI STUDI DI PADOVA

DIPARTIMENTO DI BIOLOGIA

Corso di Laurea in Scienze Naturali

ELABORATO DI LAUREA

VOLCANOLOGICAL IMPLICATIONS INFERRED FROM CHEMICAL ANALYSES OF OLIVINES COLLECTED AT SÃO JORGE ISLAND (AZOREAN ARCHIPELAGO, PORTUGAL)

Tutor: Prof. Andrea Marzoli
Dipartimento Territorio e Sistemi Agro-Forestali (TESAF)

Co-tutor: Prof. Davide Novella
Dipartimento di Geoscienze

Laureanda: Erica Luce Beghini

ANNO ACCADEMICO 2022/2023

Abstract

The Azorean Archipelago, situated in the North Atlantic Ocean, is composed of nine active volcanic islands, put in place during the Quaternary. They are a result of the interaction between the Azores hotspot and the Mid-Atlantic Ridge (MAR). The archipelago intersects the MAR, with the Western Islands situated on the ridge's western flanks, and the Central and Eastern Islands located at the east of it. This intricate setting is situated at the triple junction of the North American, Eurasian, and Nubian plates. In addition, the Terceira Rift, an exceptionally slow-spreading plate boundary, influence the archipelago's tectonics and seismicity. The Azorean plateau experiences active faults contributing to high-magnitude earthquakes, along with secondary manifestations of volcanism like fumaroles and thermal springs. Together with Madeira, the Canary Islands, and Cape Verde, the Azores constitute the Macaronesian island group. These islands are volcanic systems that result from mantle plume activity, featuring the characteristic composition of Ocean Island Basalt (OIB) magma.

This study focuses on olivine phenocrysts from the Holocene Manadas Volcanic Complex basalts on São Jorge Island, Central Azores. These crystals provide insights into magma evolution and diffusion processes. Olivine, that is commonly found in effusive alkaline mafic volcanic rocks, reacts when the magma composition changes, developing chemical zoning. Examining this zoning, both with optical mineralogy techniques and with electron microprobe analyses, made it possible to reveal the evolution of magmatic reservoirs and conduits of this volcanic complex. In addition, chemical profiles of olivine crystals and chemical diffusion modelling were used to calculate an approximate time scale of the magma evolution and eruption. We found distinct cases of both close and open-system differentiation, like magma mixing, which occurred either well before or immediately preceding eruptions. Overall, the study improves the understanding of the complex geological processes shaping the Azores and contributes to the wider field of volcanic and magmatic studies.

Table of Contents

1 Introduction

1.1 Geographical and geological setting of the Azorean Archipelago

The Azorean Archipelago consists of nine active volcanic islands located in the North Atlantic Ocean. The islands were mainly built during the Quaternary as a result of the interaction between the Mid-Atlantic Ridge (MAR) (Hildenbrand et al., 2014) and the Azores hotspot, which is caused by an upwelling mantle plume (Gente et al., 2003) (Kueppers & Beier, 2018). The islands themselves cross the MAR: the Western Islands, which include Flores and Corvo, set on the western flanks of the ridge, while the Central Islands (Faial, Pico, Graciosa, Terceira and São Jorge), and the Eastern Islands, which include São Miguel and Santa Maria, are located East of the ridge (O'Neill & Sigloch, 2018). The archipelago is located at the triple junction between North American, Eurasian and Nubian plates.

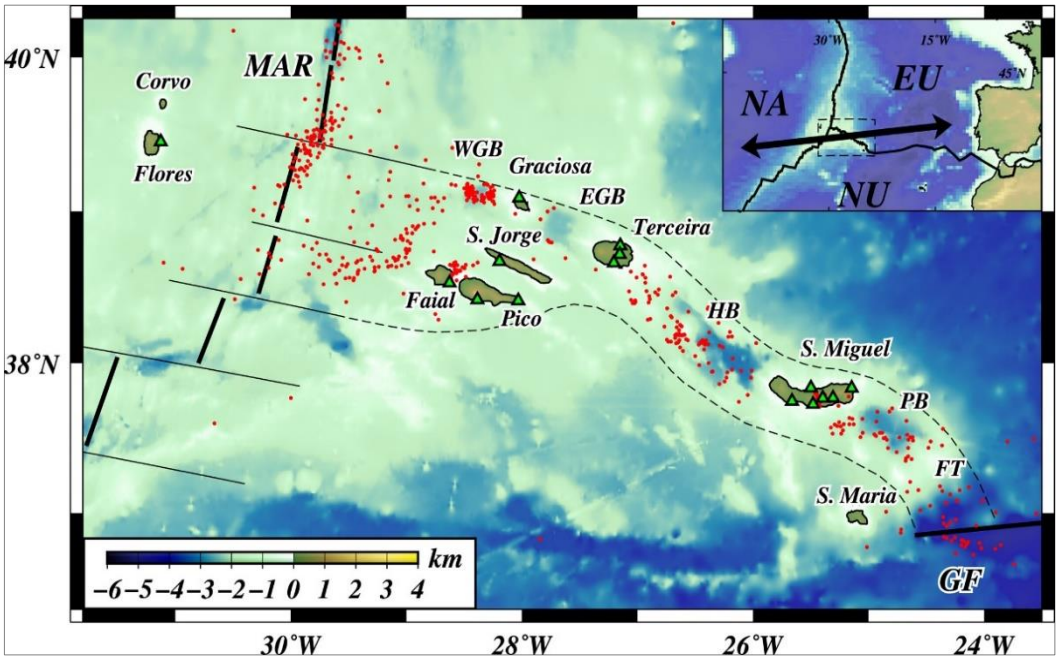

Fig. 1.1: Location of the Azores archipelago and the triple junction between North American (NA), Eurasian (EU) and Nubian (NU) plates. Green triangles are continuous GPS stations, red circles are recorded earthquakes between April 2000 and January 2017 (D'Araújo et al., 2022).

To understand the complexity of plates tectonic that affect these island, the Terceira Rift has to be taken into account: this is a 550 km long rift, considered to be the world's slowest-spreading (hyper-slow) plate boundary, with a separation rate of 4 mm/y (Vogt & Jung, 2004). Furthermore, it constitutes the northeast boundary of the eastern Azores plateau, and the divergence border between the Nubian and Eurasian plates. The movements induced by the mantle convection can account for

the rifting regime in the area, and its consequences in terms of surface morphology and seismicity (Adam et al., 2013): as the plate separates, molten material rises from the mantle, creating new basaltic crust. The process results in the formation of underwater seamounts and deep graben.

Hence, due to this composite geological setting, the Azores plateau is stressed by active faults responsible for recurrent high-magnitude earthquakes (Hildenbrand et al., 2008) (Borges et al., 2007), and by secondary manifestations of volcanism such as hydrothermal fumaroles, thermal springs and soil degassing areas (Viveiros et al., s.d.) (Caliro et al., 2015).

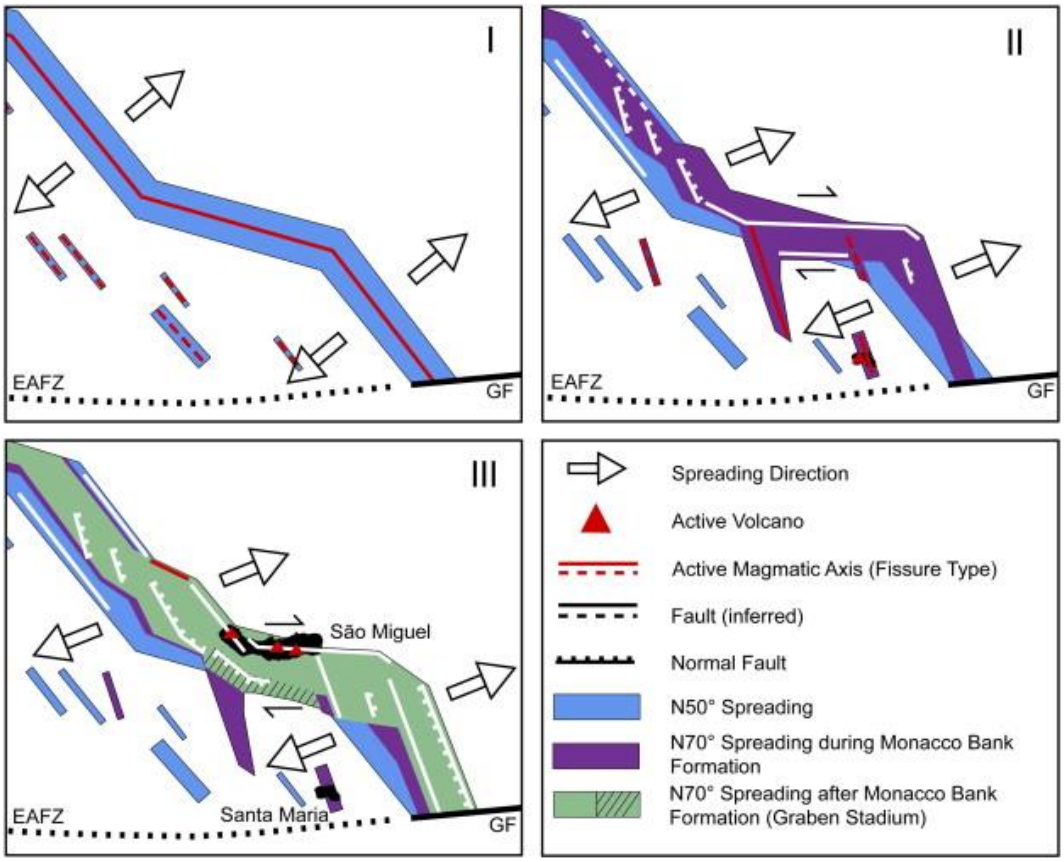

Fig. 1.2: Sketch of evolutionary stages of the southeastern Terceira Rift. Fissure type magmatism occurred synchronously southwest of the plate boundary. EAFZ: East Azores Fracture Zone; GF: Gloria Fault. (Weiß et al., 2015).

1.2 Occurrence of Ocean Island Basalts in the North Atlantic Ocean

Along with Madeira, Canary Islands and Cape Verde, the Azores are part of the Macaronesian islands, oceanic island magmatic systems believed to represent the activity of mantle plumes, with typical Ocean Island Basalt (OIB) magma composition (Carracedo & Troll, 2021). However, compared to other archipelagos, the Azores plume is relatively weak, having a quite low buoyancy flux and low rated of magma production (Courtillot et al., 2003).

Ocean Islands Basalt characteristics and peculiarities can be listed as below (Hofmann, 1997).

- Geological setting: OIBs are associated with volcanic islands and seamounts that can form island chains or clusters.
- Mantle source: OIBs are typically formed by the interaction of mantle plumes with the Earth's lithosphere, creating hotspot-related volcanic activity. They are derived from more primitive or chemically enriched mantle sources. The primitive component, typical for example of several Hawaiian or Icelandic basalts is characterized by high He isotopic ratios as well as by Sr-Nd-Pb isotopes slightly more enriched than the depleted MORB mantle which instead controls the composition of ocean ridge basalts. Enriched geochemical signatures can be found for example on islands such as Gough (South Atlantic) or Samoa (Pacific) and are generally interpreted as being due to recycling of subducted continental material (in the forms of subducted sediments or crustal slices).
- Chemical composition: OIBs are in general enriched compared to MORBs, i.e. they have higher concentrations of trace elements, in particular those elements being highly incompatible during mantle melting (for instance Ba, U, Th and REEs).
- Eruption style: OIBs can exhibit a variety of eruptive styles, ranging from effusive lava flows to more explosive eruptions, depending on factors such as the composition of the magma and the depth of the water. A typical example of a highly energetic volcanic eruption from a Macaronesian island is the one that occurred on La Palma (Canary Island, Spain) two years ago.

1.3 Geology of São Jorge Island

São Jorge is a steep volcanic elongated ridge composed of an axial chain of Hawaiian-Strombolian cinder cones, with occasional Surtseyan tuff cones, that has a sub-aerial length of about 55 km and a maximal width of only 7 km. It has a maximal elevation of 1067 m above sea level, and a total relief of about 3000 m above the Azores plateau oceanic floor (Hildenbrand et al., 2008). Magmatism here started at least 1.85 Ma ago, in the form of fissural eruptions in the East of the island, at the Serra do Topo volcanic system (Zanon & Viveiros, 2019). Volcanic activity continued through the Quaternary, possibly in phases of strong volcanic activity alternating with periods of volcanic rest. The island's sharp topography is defined by deeply incised valleys formed through the erosion of the volcanic terrain by streams and rivers, and by harsh sea cliffs, showing the effects of marine erosion.

The samples for this study were collected from the Manadas Volcanic Complex located in the central part of the island. The sampled rocks have been classified according to the Total-Alkali-Silica classification (LeBas et al., 1986) as basalts and trachybasalts (hawaiites, being sodic in composition). The complex consists in lava flows and numerous recent strombolian volcanic cones (Hildenbrand et al., 2008). Based on radiocarbon data, the volcanic activity dates back to the Holocene epoch, less than 12 Ka ago (Madeira & Brum Da Silveira, 2009). The analysed samples are specifically from prehistoric flows (Holocene) and two historical eruptions, one that occurred in 1580 CE and the other that occurred in 1808 CE.

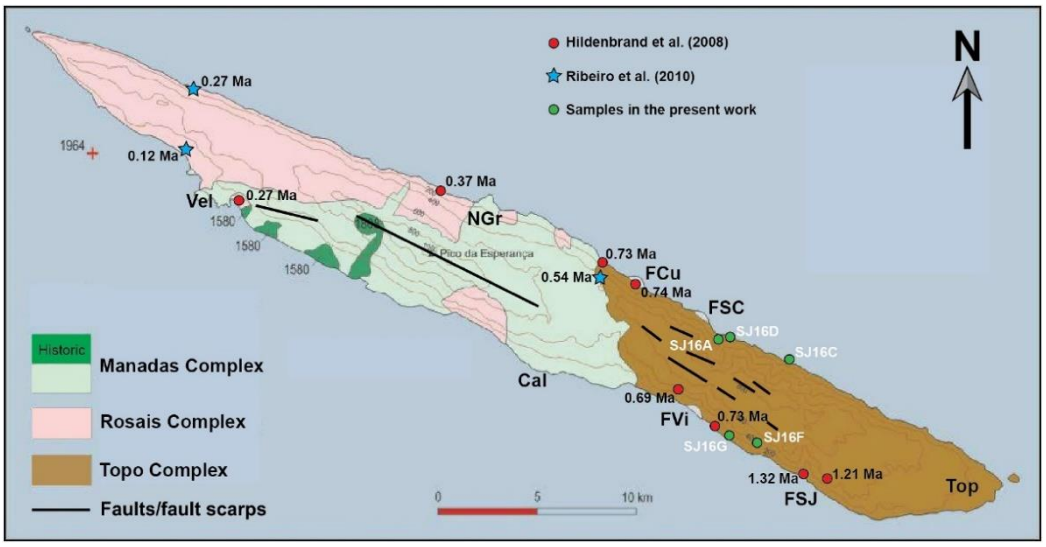

Fig. 1.3: Geological map of São Jorge showing the elongated shape of the island and the three main volcanic system with their relative age (Marques et al., 2018).

1.4 Petrographic characteristics of olivines

Olivines are a complete solid solution of magnesium iron orthorhombic nesosilicates, with the chemical formula $(Mg,Fe)_2SiO_4$. A complete isomorphous series exists, grading from the Mg-rich end member (Forsterite) to the Fe-rich end member (Fayalite) (Norman Levi Bowen & John Frank Schairer, 1935). Olivine commonly occurs as phenocrysts in volcanic rocks, where its crystal habit provides valuable insights into the magma's evolution and cooling history.

Olivines in basaltic magmas are generally quite rich in the forsteritic component (Mg_2SiO_4). At equilibrium, the Fe/Mg ratio of olivine is ca. 0.3 the Fe/Mg of the magma from which the olivine crystallizes. However, when magma mixing occurs and equilibrium conditions are disturbed, it is possible to find olivine crystals which are either more or less enriched in the forsteritic component. If the Fo content of the olivine is higher than expected (Fo > 90) for the equilibrium conditions, the olivine may be a xenocryst from the mantle or from a more mafic magma. On the contrary, Fo contents lower than equilibrium values may suggest that the olivine initially crystallized from a relatively low-MgO magma and was subsequently entrained by a more mafic magma. Core-rim chemical profiles of olivine crystals may show evidence for such processes (Roeder & Emslie, 1970).

1.5 Time scale measurement through the analysis of crystallization in olivines

The crystallization process of minerals is influenced by factors such as temperature, pressure, composition of the magma, and the rate of cooling. In general, crystals nucleate and then grow starting from the liquidus temperature. In the case of olivine, this temperature corresponds to about 1250-1300 °C in the studied magmas. Zoning (chemical and optical variations) can occur when crystals experience a change of the surrounding magma composition, which gets either more evolved, lower in Mg in a closed system environment, or less evolved (more primitive), when new mafic magma is added to the magmatic system in an open system environment. An example of zoning may result also from fluctuating environmental conditions, that lead to the creation of distinct concentric bands within their structure. The zoning patterns of crystals are a valuable source of information that can be used to reconstruct the processes which occurred in magmatic reservoirs and volcanic

conduits. Analyses of the mineral zoning and modeling based on chemical diffusion laws also allows the determination of the durations and rates of some magmatic processes (Costa et al., 2008).

Chemical diffusion occurs when the crystal is out of equilibrium with the surrounding magma. This may happen in a closed or open system. In the case of olivine, Mg and Fe diffuse out or into the crystal to adapt to the new composition. Mg and Fe diffusion need to be mutually compensated (Mg replaces Fe and viceversa). Such diffusion process in olivine is quite fast, at high temperature, but it depends also on the crystallographic orientation of the crystal, varying by almost a factor 10 along the 3 main axes in olivine. Diffusion is strongly controlled by temperature, being fast at high magmatic T (1200-1300 °C), while it gets sluggish at low T, for example during rise of the magma and then during eruption. It can be considered that immediately after eruption, the diffusion process is completely stopped.

In this study the diffusion process of a few olivine crystals were modelled, following the diffusion coefficient in olivine for Mg and Fe calculated by Girona & Costa, (2013):

$$D_{[001]} = 10^{-9.21} * \left(\frac{fO_2}{10^{-7}}\right)^{\frac{1}{6}} * 10^{3(0.9-X_{Fo})} * \exp\left(-\frac{E_{Fo} + 7 * 10^{-6} * (p - 10^5)}{RT}\right)$$

This equation shows that the diffusion speed is controlled also by the oxidation state (oxygen fugacity) of the magmas. This can correspond to the Quartz-Fayalite-Magnetite buffer, it a moderately oxidizing condition typical of OIBs. The olivine crystallization temperature is set at 1250 °C, as resulting from clinopyroxene geo-thermometry (Marzoli, personal communication).

Different chemical profiles and different core compositions of zoned olivine crystals suggest that they formed from slightly distinct melts that were mixed in origin. The major elements of olivine (Mg and Fe) tend to adapt to the changing melt composition by diffusive re-equilibration. Therefore, profiles of these

elements can be used to evaluate the time elapsed since the magma mixing event and the freezing of the system caused by the eruption of the magmas (Marzoli et al., 2015).

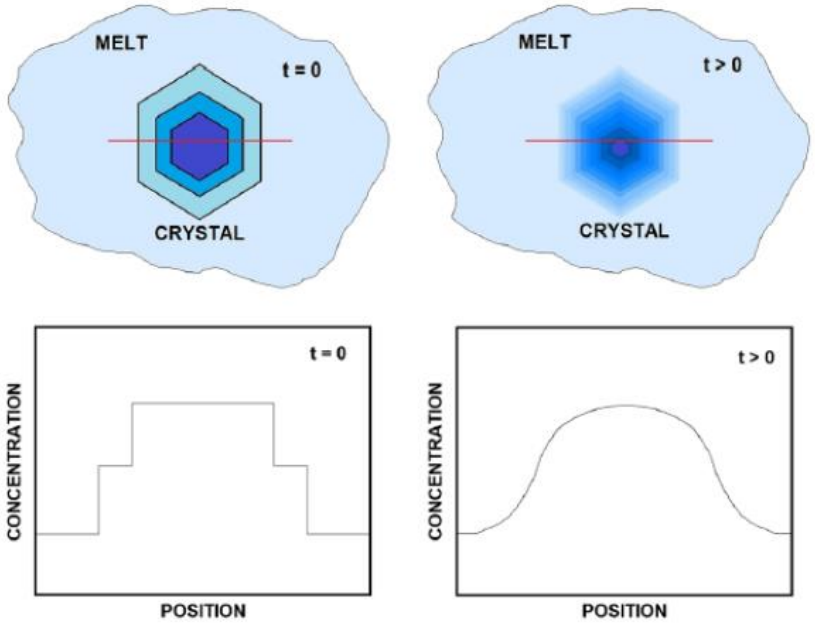

Fig. 1.4: The left-side panel show the optical (top left) and chemical (bottom-left) zoning of an olivine crystal, without evident diffusive re-equilibration. The right-side panels show instead a crystal which experienced a partial diffusive re-equilibration. Notably, complete re-equilibration would result in a olivine without optical and chemical zoning and compositions fully in equilibrium with the surrounding melt (or matrix) (Girona and Costa, 2013).

1.6 Aim of the study

This study focuses on the chemical analysis of olivine phenocrysts found in Manadas basalts, with the aim to extract data than fit with the diffusive re-equilibration model, that could offer an opportunity to investigate the magmatic processes of the area and their time scales.

2 Materials and methods

2.1 Sample collection and preparation

Rocks for this thesis were sampled along the western part of the São Jorge island, where the Holocene products were erupted. Focus was given in particular on the only 2 known sub-aerial historic eruptions of the island (1580 and 1808 CE; note that the island was probably settled in the XIV and XV century). After collecting the rock samples, these were cut with a diamond saw to obtain thin slivers, that

were subsequently flattened and mounted on a glass slide. They resulted in six petrographic thin sections of ca 4x2 cm in size with a thickness of 30 microns: AJ78, AJ79 from the 1580 CE eruption, AJ77 and AJ83 form the 1808 eruption CE, while AJ76 and AJ81 were sampled from prehistoric Holocene flows. Thin sections were then polished to be suitable for microscopy and EMPA analyses.

2.2 Petrographic microscopy examinations

The most appropriate olivine crystals for EMPA analyses were previously examined through optical mineralogy, and must had the following characteristics:

- a size larger than 200 microns (maximum axis);
- a regular shape, subhedral to euhedral;
- as few fractures as possible.

Under plane polarized light, phenocrysts appeared as colourless, with high relief, absent pleochroism, absent cleavage and common irregular fractures, whereas, under cross polarized light, they could be easily recognized by bright interference colours (II°-III° order) and by parallel extinction angle.

Crystals that fitted with these criteria were numbered and photographed, both in PPL and XPL mode: a total of 12 olivines from all the thin sections were selected.

Fig. 2.1: Thin section AJ79 under PPL. A colourless olivine is visible in the higher left quadrant.

Fig. 2.2: Thin section AJ79 under XPL. Olivine in the higher left quadrant appears now as bright green.

2.3 Electron probe microanalyzer (EMPA) analyses

Mineral major and minor element compositions were analysed at Milano University (Italy), with a JEOL JXA 8200 Superprobe at 15 nA and 15 kV. Natural and synthetic standards were used. This electron microprobe can determine the chemical composition of solid material through the emission of an electron beam: the electrons collide with the atoms in the specimen, thus emitting electromagnetic waves of various energies, among which characteristic X-rays. The chemical composition is determined by comparing the intensities of the characteristic X-rays from the specimen with intensities of known composition (standards) (Lewis et al., 2012).

For each phenocryst, a straight line was tracked from the core to the border, and measurements were performed under an electron beam of ca. 1 micron in diameter, with a distance between successive analytical spots of 5 microns. Each spot was numbered. Sample AJ76 was not analysed. Only 72 of the 164 planned spots for olivine 8 of sample AJ81 were measured, because of machine malfunctioning.

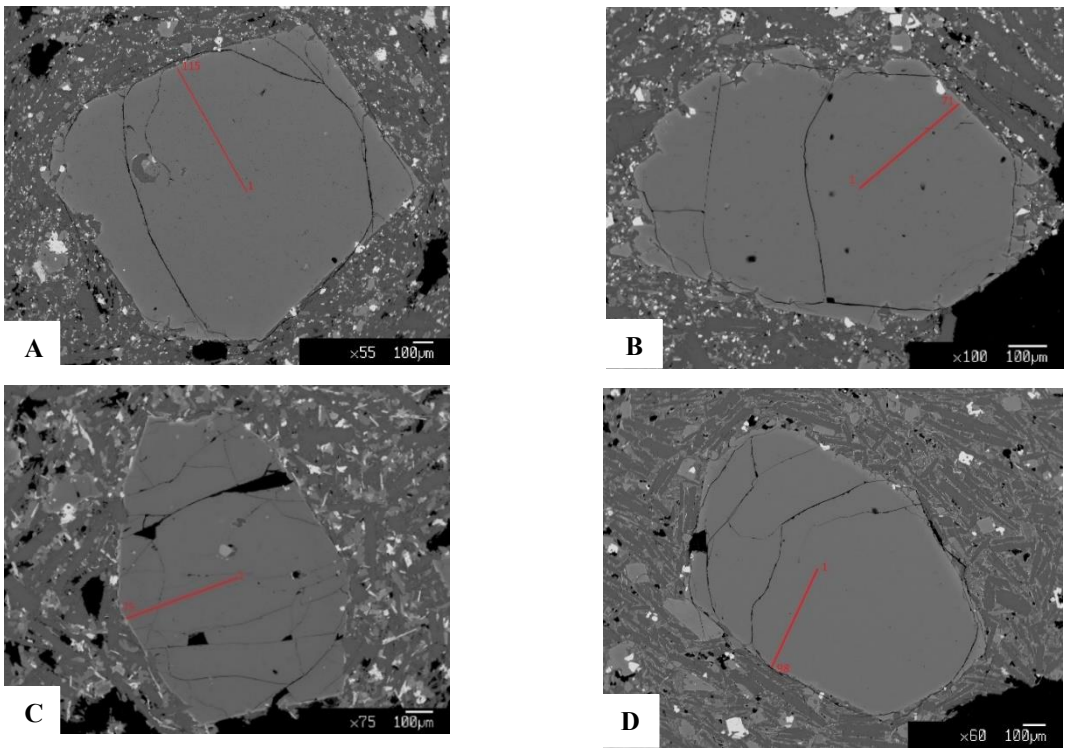

Fig 2.3: microphotographs taken with EMPA of analysed phenocrysts. Red lines link the analytical spots. A: Olivine 2 of sample AJ77; B: Olivine 4 of sample AJ79; C: Olivine 6 of sample AJ81; D: Olivine 6 of sample AJ83.

2.4 Data analyses

Percentages by weight of the major element oxides obtained through EMPA were then used to calculate Forsterite/Fayalite components for all the analysed crystals. A graph with the total amount of Forsterite for every spot analysed was plotted for each olivine.

3 Results

3.1 Petrography

The petrographic microscopy revealed that sampled rocks are frequently vesicular and exhibit aphanitic and glassy groundmasses. They contain phenocrysts and microphenocrysts usually isolated and sometimes in the form of glomeroporphyritic aggregates.

Mineral assemblages consist essentially of olivine, plagioclase and clinopyroxene occurring as phenocrysts, microphenocrysts and groundmass crystals. The groundmass is primarily made up of plagioclase laths, Fe-Ti oxides, and very rare amphibole (in AJ77). Phenocrysts are mainly subhedral and unresorbed, yet occasionally they may show slightly to strongly resorbed margins, typically in plagioclase and clinopyroxene. Optical zoning is well developed in some plagioclase and clinopyroxene crystals (light brown cores to reddish brown rims), while olivine crystals lack of significant evidence for zoning.

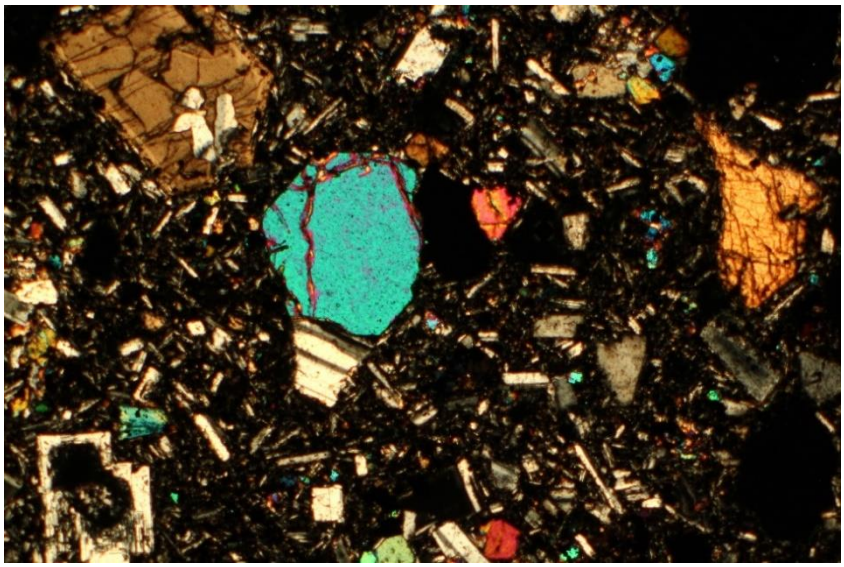

Fig. 3.1: microphotograph of a portion of sample AJ76, where it is possible to appreciate olivine and clinopyroxene phenocrysts and microphenocrysts surrounded by the aphanitic groundmass of plagioclase laths.

3.2 Olivine chemistry

Representative olivine chemical compositions obtained by EMPA are summarized in Table 1.

Sample	Crystal	Zone	MgO	SiO_2	CaO	MnO	FeO	NiO	Fo	Fa
AJ77	Olivine 2	Core -0	40.48	39.47	0.2	0.31	21.33	0.04	76.92	22.73
		Core -5	40.25	39.25	0.21	0.25	21.3	0.11	76.89	22.82
		Core -10	38.93	40.65	0.19	0.22	21.1	0.02	76.49	23.26
		Rim-560	38.57	38.73	0.21	0.38	23.25	0.03	74.41	25.16
		Rim-565	38.33	38.56	0.21	0.41	23.84	0	73.80	25.75
		Rim-570	37.53	38.43	0.22	0.61	25.13	0.01	72.20	27.12
AJ78	Olivine 2a	Core -0	39.68	39.20	0.19	0.32	21.84	0.05	76.14	23.51
		Core -5	39.79	39.29	0.19	0.28	21.97	0.09	76.11	23.57
		Core -10	40.32	39.10	0.17	0.28	21.78	0.09	76.50	23.18
		Rim-355	40.01	39.29	0.23	0.32	21.92	0.05	76.22	23.43
		Rim-360	39.73	39.3	0.23	0.34	21.9	0.05	76.09	23.53
		Rim-365	39.77	39.06	0.22	0.33	22.7	0.09	75.47	24.17
	Olivine 2b	Core -0	39.78	39.45	0.22	0.26	21.68	0.03	76.36	23.34
		Core -5	40.2	39.14	0.2	0.25	21.73	0.08	76.52	23.20
		Core -10	40.46	39.26	0.18	0.28	21.9	0.04	76.47	23.22
		Rim-260	37	38.66	0.25	0.44	25.74	0.06	71.58	27.93
		Rim-265	36.78	38.3	0.27	0.4	26.3	0.01	71.05	28.50
		Rim-270	35.4	38.14	0.28	0.43	27.48	0.02	69.32	30.19
	Olivine A	Core -0	39.96	39.04	0.19	0.30	21.55	0.05	76.52	23.15
		Core -5	40.43	39.02	0.22	0.31	21.99	0.0745	76.36	23.30
		Core -10	40.37	39.52	0.19	0.31	21.64	0.1423	76.62	23.04

		Rim-360	37.09	38.9	0.31	0.38	25.69	0.06	71.71	27.86
		Rim-365	34.02	37.73	0.4	0.48	29.4	0.05	66.98	32.47
		Rim-370	27.56	36.5	0.42	0.76	36.21	0.04	57.05	42.05
AJ79	Olivine 4	Core-0	40.21	38.83	0.18	0.19	21.12	0.07	77.07	22.71
		Core-5	40.31	39.29	0.17	0.25	21.35	0.07	76.88	22.84
		Core-10	40.27	38.82	0.18	0.32	21.46	0.08	76.72	22.93
		Rim-340	38.65	38.31	0.23	0.33	23.78	0.036	74.074	25.56
		Rim-345	37.37	37.92	0.27	0.48	25.41	0.02	72.01	27.46
		Rim-350	34.1	37.78	0.33	0.54	29.09	0.01	67.22	32.17
	Olivine 7	Core-0	41.79	39.8	0.21	0.28	20.2	0.08	78.43	21.26
		Core-5	41.26	39.45	0.21	0.25	19.8	0.07	78.57	21.15
		Core-10	41.33	39.41	0.19	0.26	20.04	0.11	78.39	21.32
		Rim-870	39.39	38.67	0.24	0.45	22.16	0.01	75.64	23.87
		Rim-875	37.68	38.78	0.25	0.43	24.21	0	73.15	26.37
		Rim-880	35.58	38.17	0.37	0.65	27.14	0.02	69.52	29.75
AJ81	Olivine 2	Core-0	40.87	39.44	0.18	0.29	20.58	0.12	77.73	21.96
		Core-5	41.21	39.17	0.2	0.28	20.42	0.15	78.01	21.68
		Core-10	41.06	39.18	0.18	0.28	20.31	0.13	78.04	21.65
		Rim-755	42.67	40.05	0.26	0.21	17.47	0.15	81.13	18.63
		Rim-760	42.88	39.84	0.26	0.22	17.61	0.14	81.08	18.68
		Rim-765	42.55	39.77	0.26	0.26	18.08	0.15	80.52	19.19
	Olivine 6	Core-0	42.44	39.34	0.19	0.22	18.5	0.18	80.15	19.60
		Core-5	42.26	39.41	0.22	0.24	18.8	0.14	79.82	19.92
		Core-10	42.31	39.45	0.18	0.22	18.53	0.15	80.08	19.67

		Rim-360	42.55	40.04	0.24	0.21	17.68	0.12	80.91	18.85
		Rim-365	42.34	39.62	0.24	0.24	17.98	0.14	80.55	19.19
		Rim-370	42.42	39.84	0.22	0.22	18.42	0.11	80.22	19.54
	Olivine 8	Core-0	40.75	39.39	0.17	0.23	20.92	0.09	77.44	22.30
		Core-5	40.64	38.94	0.21	0.24	20.73	0.09	77.55	22.19
		Core-10	40.54	39.27	0.19	0.34	20.77	0.09	77.39	22.24
		Rim-345	40.52	39.25	0.2	0.28	21.05	0.03	77.19	22.49
		Rim-350	40.19	39.35	0.2	0.23	20.9	0.04	77.22	22.52
		Rim-355	40.7	38.8	0.21	0.23	20.51	0.10	77.76	21.98
AJ83	Olivine 2	Core-0	40.42	39.04	0.2	0.25	19.19	0.11	78.75	20.97
		Core-5	40.38	38.64	0.19	0.28	19.48	0.14	78.46	21.23
		Core-10	40.5	38.66	0.19	0.2	19.27	0.14	78.75	21.02
		Rim-385	37.7	38.27	0.21	0.41	22.98	0.06	74.18	25.36
		Rim-390	36.65	38.19	0.19	0.38	24.49	0.02	72.42	27.15
		Rim-395	36.04	37.88	0.23	0.48	24.84	0.09	71.72	27.73
	Olivine 3	Core-0	40.36	38.77	0.17	0.34	20.81	0.05	77.28	22.35
		Core-5	39.89	38.66	0.18	0.27	20.91	0.11	77.04	22.65
		Core-10	39.8	39.18	0.15	0.33	20.61	0.06	77.20	22.43
		Rim-290	38.87	38.55	0.21	0.42	22.25	0.03	75.34	24.19
		Rim-295	38.05	38.15	0.2	0.40	23.07	0.01	74.29	25.27
		Rim-300	37.47	37.88	0.24	0.48	23.9	0.03	73.25	26.21
	Olivine 4	Core-0	40.18	38.98	0.18	0.22	21.1	0.03	77.06	22.70
		Core-5	40.07	39.17	0.16	0.22	21.31	0.06	76.83	22.92
		Core-10	40.11	38.88	0.2	0.22	21.02	0.01	77.09	22.66

		Rim-475	40.01	38.75	0.19	0.31	20.91	0.02	77.06	22.59
		Rim-480	39.14	39.03	0.21	0.28	21.77	0.02	75.98	23.71
		Rim-485	38.05	38.69	0.23	0.37	23.48	0.02	73.98	25.61

Table 1: wt% of major oxides and Fo/Fa contents measured for the first and the last three spots of each phenocryst. Note that the totals for all reported analyses vary between 100.0 and 102.9 wt%.

3.3 Forsterite profiles

Graphs relating the Fo content (ordinate) to the distance from the core (abscissa) in microns for each olivine are reported below. Outliers are to be interpreted as spots where the measurement is less accurate, due to fractures or inclusions in the crystal.

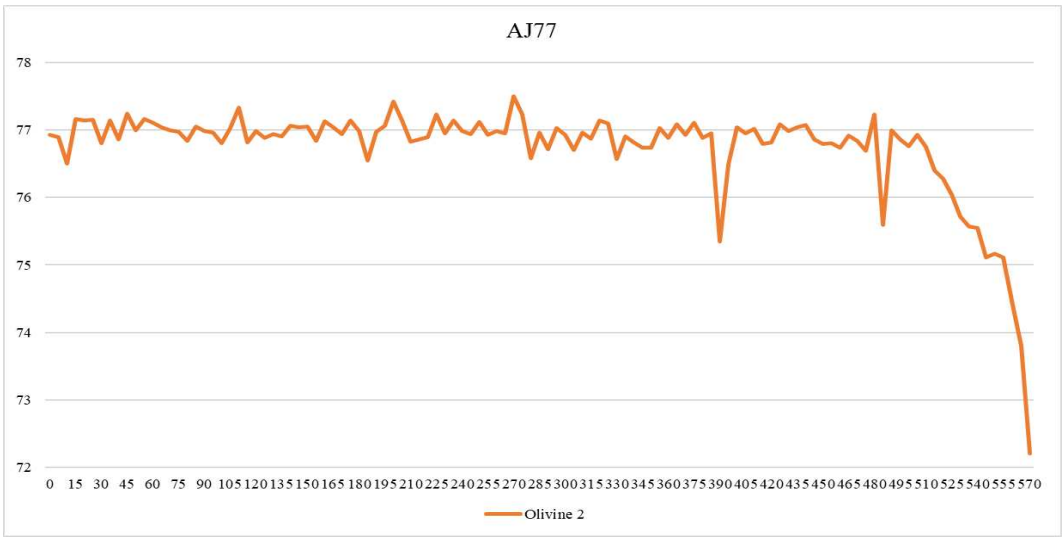

Fig. 3.2: Forsterite content in the only olivine analysed for sample AJ77.

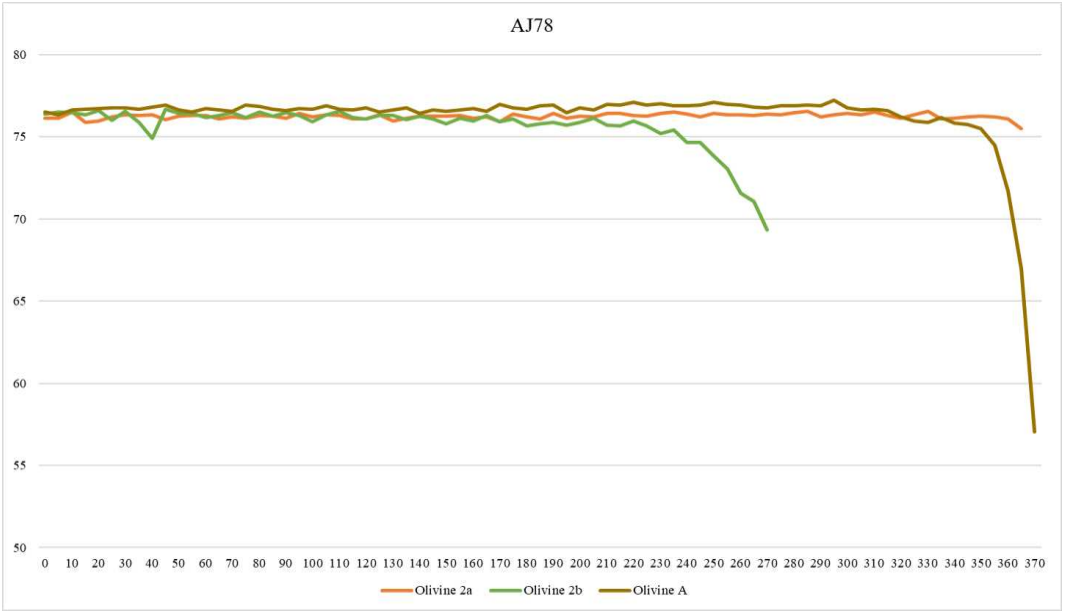

Fig. 3.3: Forsterite contents in three olivines analysed for sample AJ78.

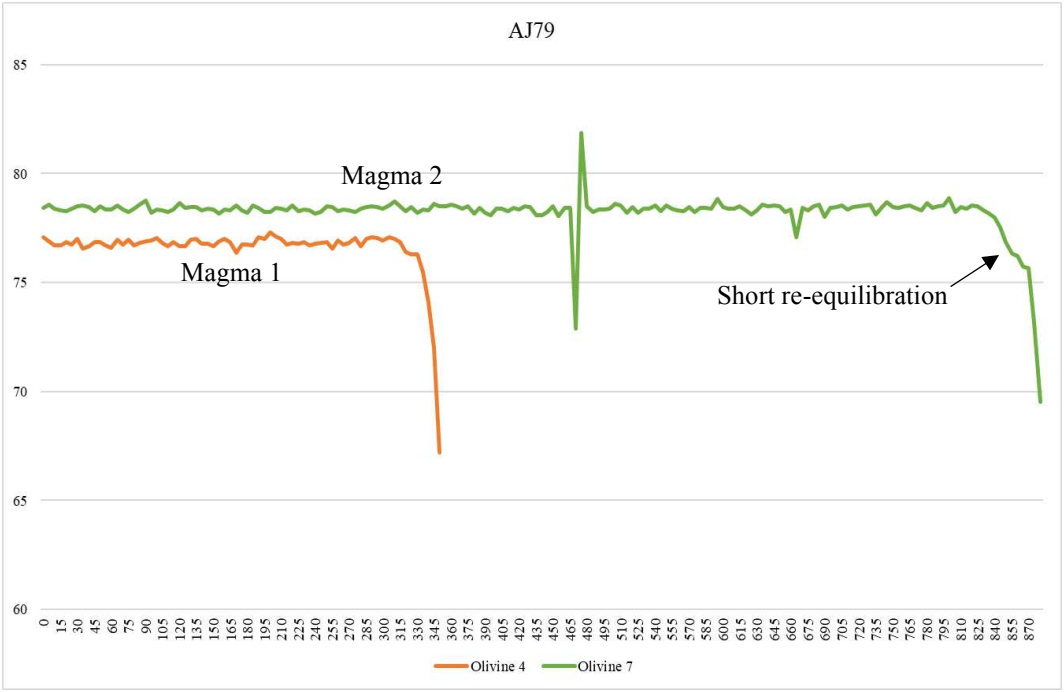

Fig. 3.4: Forsterite contents in two olivines analysed for sample AJ79.

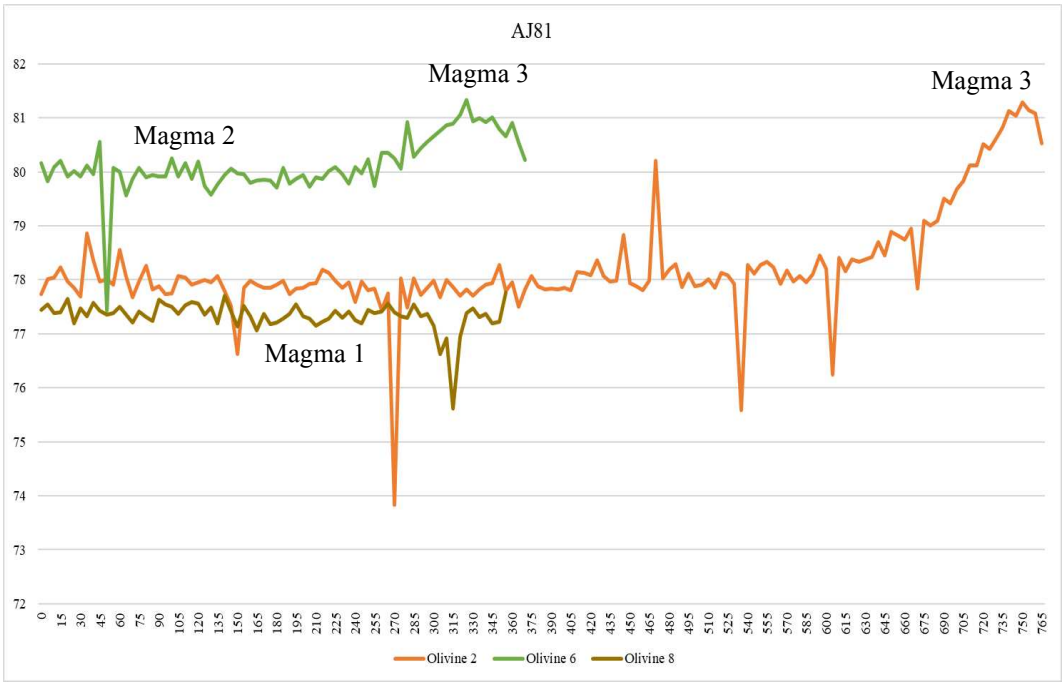

Fig. 3.5: Forsterite contents in three olivines analysed for sample AJ81.

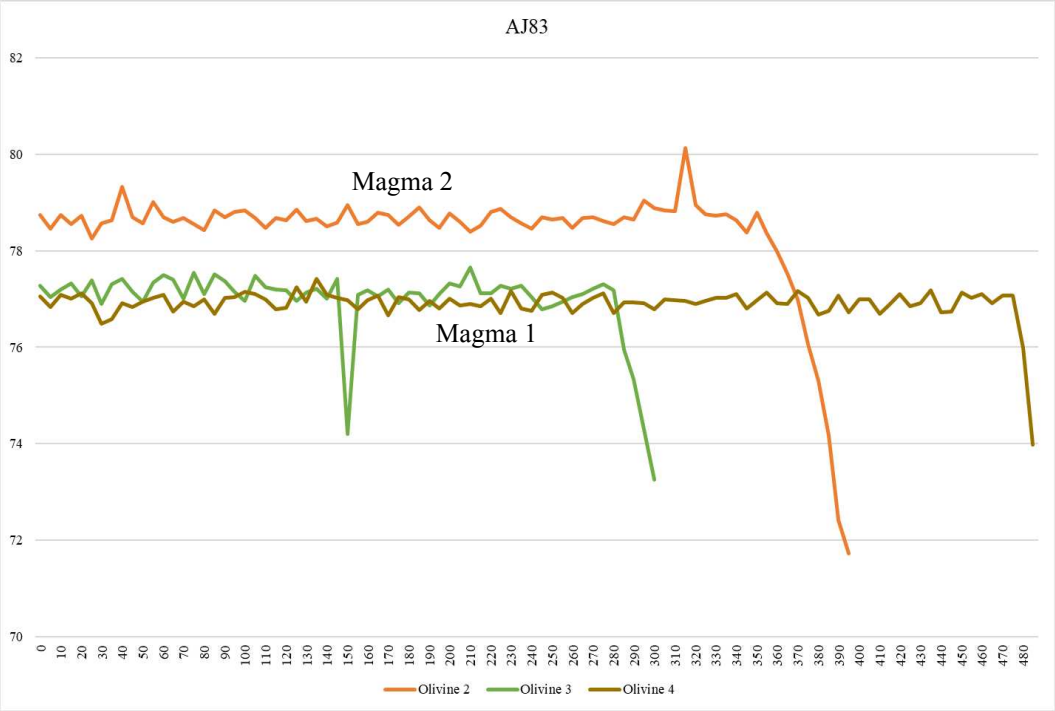

Fig. 3.6: Forsterite contents in three olivines analysed for sample AJ83.

3.4 General trends

Most of the profiles (thin sections AJ77, AJ78, AJ79 and AJ83) are flat (constant Fo), with a trend that sees the Forsterite content (and therefore Mg) dropping as the measurements approach the rim, down to a minimum of Fo_{57} in Olivine A of thin section AJ78. However, a peculiar case is represented by thin section AJ81, where instead a progressive rim-ward enrichment of Forsterite content is observed, up to a maximum of Fo_{81} at the rim of Olivine 6.

Also, in both AJ81 and AJ83 samples distinct groups of olivine compositions can be seen. In each thin section, olivine core from distinct crystals differs by at least 2% of Forsterite: this is clear evidence of crystals generated by different magmas (mixing). In both samples the olivine core-rim profile shows no evidence of re-equilibration, except at the outermost rims.

In AJ79 sample, the two phenocrysts are slightly different: Forsterite in Olivine 7 descends from $Fo_{78.5}$ to about Fo_{77}, where it stops and shows a stable composition for some microns, that corresponds quite well with the Forsterite content of the core of Olivine 4 (ca. Fo_{77}).

4 Discussion

4.1 Close-system differentiation: fractional crystallization

This process is related to isolated magma reservoirs beneath a volcano, that is cut off from external influences such as the influx of new magma. As the magma cools, minerals begin to crystallize, with olivine generally being the first crystallizing phase at the liquidus. In such environment, the magma may evolve to more differentiated, less dense and more volatile-element enriched compositions eventually being erupted.

Some of the olivine crystals analysed in this study (for instance, those from sample AJ78 and possibly those from sample AJ77) probably come from this type of magmatic system, since they gradually reach a lower composition in Fo which is the result of fractional crystallization: the magma slowly becomes more and more depleted of Mg. Distinct olivine crystals from the same sample yield almost identical Fo contents and core-rim compositional profiles.

4.2 Open-system differentiation: magma mixing

Magma chambers may be also subject to the intrusion of new magma, and when magmas from different sources mix, they can undergo chemical reactions and physical interactions, that can lead to changes in the mineralogy and chemistry of the resulting material. Magma mixing and recharge of new, primitive, hot magma can influence the eruption behaviour and style of volcanic activity as well.

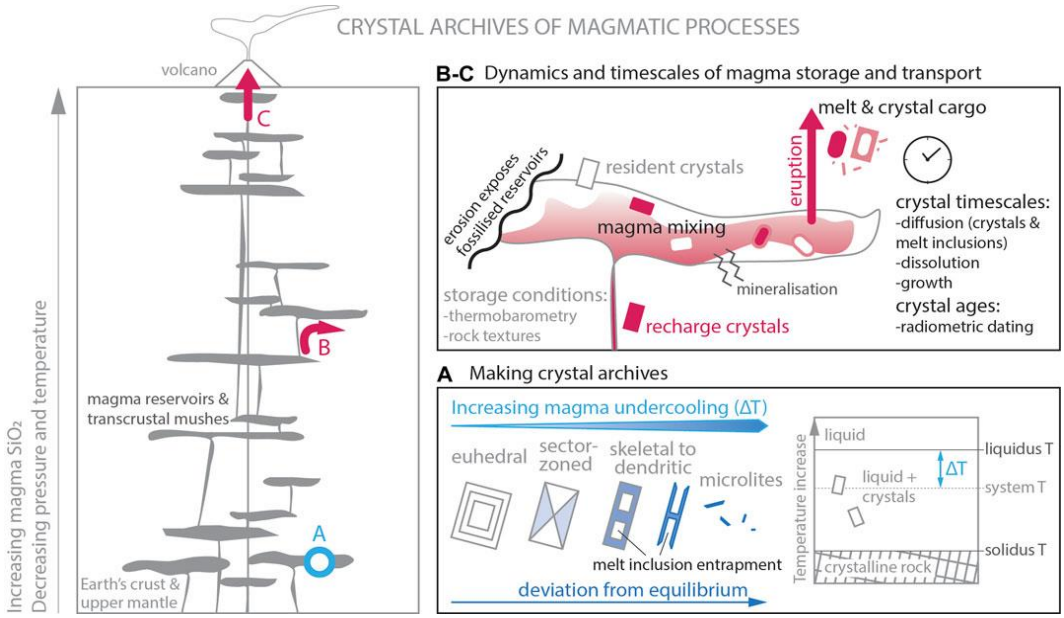

Figure 4.1: magma plumbing systems. A: variations in crystal shape, zoning style and melt inclusions with the increase in magma undercooling. B: crystals record the dynamics of magma storage and transport between reservoirs, including magma mixing. C: timescales can be reconstructed by considering limitations on the rates of crystal growth, dissolution, and diffusive re-equilibration. (Ubide et al., 2021).

According to Ubide et al. (2021), most Ocean Island Basalts are the product of open system processes in the deep oceanic crust, where magma rising from the mantle differentiates and acquires a cargo of previously crystallized minerals. Sample AJ81 brings the evidence that, for that peculiar prehistoric Holocene eruption, there was a contact in the magmatic plumbing system with magma enriched in Mg, which allowed olivine to crystallize more Fo-rich compositions at the rim rather than in the core of the olivine crystals. Moreover, data confirm the increase in the Forsterite content within the outermost 150 microns of the crystals. This implies that magma mixing took place before the eruption, and could potentially have served as a triggering factor for the eruption.

Olivine crystals from AJ79 and AJ83 show normal zoning, but distinct crystals within a same thin section show markedly distinct Fo contents in the crystal cores. Such evidence suggests an open-system process for these magmas. In particular, the most Fo-rich olivine of AJ83 (Olivine 2) tends to briefly re-equilibrate with the more Fa-rich composition of the other olivine crystal (Olivine 3 and Olivine 4). This suggests that the relatively Mg-rich and Mg-poor magmas from which the three olivine cores crystallized got mixed very shortly before the eruption. Instead,

in the case of AJ79, the two analysed olivine crystals show slightly distinct core compositions and lack any evidence of re-equilibration. In this case the mixing event must have occurred immediately before the eruption, not allowing for re-equilibration.

4.3 Diffusion modelling and residence times before eruption

Semi-quantitative diffusion modelling was done after Girona & Costa, (2013). This method requires input of T and fO_2 values. These parameters were obtained from clinopyroxene geothermometry (following Neave & Putirka, 2017) and ilmenite-magnetite oxybarometry. Since information on the olivine crystallographic orientation is lacking, there are significant uncertainties on the obtained results. For this reason, the longest equilibration times are described in the following paragraphs. Three distinct diffusion re-equilibration scenarios could be defined:

1. the case of sample AJ81. Here mixing of three distinct magmas occurred at least 6 months before the eruption. The low-Fo olivine crystals (Olivine 2 and Olivine 8) initially formed from Magma 1, while the Fo-rich olivine (Olivine 6) crystallized from a more Mg-rich Magma 2. These magmas were not in contact until Magma 3 fluxed the system. It can be proposed that Magma 1 was shallower than Magma 2. Magma 3 was the most Mg-rich one. Olivine crystals tended to re-equilibrate with Magma 3, and this process may have lasted up to 6 months.
2. the case of sample AJ79. Based on the obtained data, the two analysed olivine crystallized from two distinct magmas. It is possible that the low-Fo olivine (Olivine 4) was residing at a relatively shallow depth in the magmatic system and crystallized from Magma 1. A new batch of magma, Magma 2, reached this level, carrying the Fo-rich olivine (Olivine 7). This latter shows subtle evidence of rapid re-equilibration with Magma 1. The lack of such re-equilibration in the low-Fo crystal may suggest that Magma 1 was volumetrically dominant. Modelling of the Fo variation in the high-Fo crystal indicates that the mixing process occurred in a maximum of few days (2-3) before the eruption.
3. the case of sample AJ83. In this case, the three olivine crystals with distinct Fo content lack any evidence of re-equilibration. This indicates that the two

magmas from which the two low-Fo (Olivine 3 and Olivine 4) and the single high-Fo (Olivine 2) olivines crystallized got in contact immediately (hours?) before the eruption.

5 Conclusions

The study of olivine phenocrysts from basalts of the Manadas Volcanic Complex on São Jorge Island (Azores) provided insights into the magmatic system of the island. The Azorean Archipelago's geological setting was shaped by the interaction between the Mid-Atlantic Ridge and the Azores hotspot, which created a complex tectonic environment with active faults, high-magnitude earthquakes, and secondary manifestations of volcanism. Also, the formation and eruption styles of OIBs, which include Azorean magmas, are influenced by the interactions between mantle plumes, magma sources and lithospheric structures. Investigation of olivine crystals' chemical compositions and zoning patterns could elucidate the evolutionary history of the magmas at São Jorge Island. By examining zoned core-rim variations and diffusion processes, it was possible to semi-quantitatively constrain the timescales and evolution of the plumbing system. The study revealed both closed and open-system differentiation processes, where magma mixing plays a crucial role, since it leads to variations in chemical composition of the crystallizing minerals and could possibly trigger new eruptions.

In terms of risk containment, studies of this kind can help understand the potential danger of future eruptions and the timeframe available to the population for implementing evacuation strategies. Together with data on seismicity, degassing, tremors and ground deformation, it could be possible to draw conclusions about the speed of magma eruption following mixing events and provide insights into the regularity of these phenomena. As observed in the most recent eruption of this kind in La Palma in 2021, indications of an imminent lava outbreak were recorded based on seismic and degassing data already one year prior to the event. Furthermore, the evolution of seismic activity in the area was constantly monitored and began to change even five years before the eruption (Del Fresno et al., 2023) . It is desirable that all these data would be monitored in the Azores as well, especially because, as indicated by this study, the eruptive event could occur even within shorter

timeframes once the mixing event takes place. One worrisome conclusion of the study is in fact that the behaviour of the São Jorge magmatic system is highly variable, indicating residence times of the basaltic magmas that vary from hours to months. This hinder prediction of future eruptions, indicating that, for example, evidence of seismic tremors related to magma rise in the crust should be taken as a very serious alarm, as they may rapidly lead to magma outbreak. Moreover, assessment of volcanic risk should consider that all recent eruptions happened in the western part of the and that the highly explosive initial phases of historic eruptions (1580 and 1808 CE) did cause tens of casualties (Zanon & Viveiros, 2019).

To sum up, this study not only gives additional tools for the comprehension of Azores' volcanic history, but it could also provide information on the behaviour of similar oceanic island systems.

References

Adam, C., Madureira, P., Miranda, J. M., Lourenço, N., Yoshida, M., & Fitzenz, D. (2013). Mantle dynamics and characteristics of the Azores plateau. *Earth and Planetary Science Letters*, *362*, 258–271.

Borges, J. F., Bezzeghoud, M., Buforn, E., Pro, C., & Fitas, A. (2007). The 1980, 1997 and 1998 Azores earthquakes and some seismo-tectonic implications. *Tectonophysics*, *435*(1–4), 37–54.

Caliro, S., Viveiros, F., Chiodini, G., & Ferreira, T. (2015). Gas geochemistry of hydrothermal fluids of the S. Miguel and Terceira Islands, Azores. *Geochimica et Cosmochimica Acta*, *168*, 43–57.

Carracedo, J. C., & Troll, V. R. (2021). North-East Atlantic Islands: The Macaronesian Archipelagos. In *Encyclopedia of Geology* (pp. 674–699). Elsevier.

Costa, F., Dohmen, R., & Chakraborty, S. (2008). Time scales of magmatic processes from modeling the zoning patterns of crystals. *Reviews in Mineralogy and Geochemistry*, *69*(1), 545–594.

Courtillot, V., Davaille, A., Besse, J., & Stock, J. (2003). Three distinct types of hotspots in the Earth's mantle. *Earth and Planetary Science Letters*, *205*(3–4), 295–308.

D'Araújo, J., Sigmundsson, F., Ferreira, T., Okada, J., Lorenzo, M., & Silva, R. (2022). Plate Boundary Deformation and Volcano Unrest at the Azores Triple Junction Determined From Continuous GPS Measurements, 2002–2017. *Journal of Geophysical Research: Solid Earth*, *127*(1).

Del Fresno, C., Cesca, S., Klügel, A., Domínguez Cerdeña, I., Díaz-Suárez, E. A., Dahm, T., García-Cañada, L., Meletlidis, S., Milkereit, C., Valenzuela-Malebrán, C., López-Díaz, R., & López, C. (2023). Magmatic plumbing and dynamic evolution of the 2021 La Palma eruption. *Nature Communications*, *14*(1), 358. h

Gente, P., Dyment, J., Maia, M., & Goslin, J. (2003). Interaction between the Mid-Atlantic Ridge and the Azores hot spot during the last 85 Myr: Emplacement and rifting of the hot spot-derived plateaus. *Geochemistry, Geophysics, Geosystems*, *4*(10).

Girona, T., & Costa, F. (2013). DIPRA: A user-friendly program to model multi-element diffusion in olivine with applications to timescales of magmatic processes. E. *Geochemistry, Geophysics, Geosystems*, *14*(2), 422–431.

Hildenbrand, A., Madureira, P., Marques, F. O., Cruz, I., Henry, B., & Silva, P. (2008). Multi-stage evolution of a sub-aerial volcanic ridge over the last 1.3 Myr: S. Jorge Island, Azores Triple Junction. *Earth and Planetary Science Letters*, *273*(3–4), 289–298.

Hildenbrand, A., Weis, D., Madureira, P., & Marques, F. O. (2014). Recent plate re-organization at the Azores Triple Junction: Evidence from combined geochemical and geochronological data on Faial, S. Jorge and Terceira volcanic islands. *Lithos*, *210–211*, 27–39.

Hofmann, A. W. (1997). Mantle geochemistry: The message from oceanic volcanism. *Nature*, *385*(6613), 219–229.

Kueppers, U., & Beier, C. (A c. Di). (2018). *Volcanoes of the Azores: Revealing the Geological Secrets of the Central Northern Atlantic Islands*. Springer Berlin Heidelberg.

LeBas, M. J. L., Maitre, R. W. L., Streckeisen, A., Zanettin, B., & IUGS Subcommission on the Systematics of Igneous Rocks. (1986). A Chemical Classification of Volcanic Rocks Based on the Total Alkali-Silica Diagram. *Journal of Petrology*, *27*(3), 745–750.

Lewis, B. J., Thompson, W. T., & Iglesias, F. C. (2012). 2.20—Fission Product Chemistry in Oxide Fuels. In R. J. M. Konings (A c. Di), *Comprehensive Nuclear Materials* (pp. 515–546). Elsevier.

Madeira, J. & Brum Da Silveira, A. (2009). Active tectonics and first paleoseismological results in Faial, Picoand S. Jorge islands (Azores, Portugal). *Annals of Geophysics*, *46*(5).

Marzoli, A., Aka, F. T., Merle, R., Callegaro, S., & N'ni, J. (2015). Deep to shallow crustal differentiation of within-plate alkaline magmatism at Mt. Bambouto volcano, Cameroon Line. *Lithos*, *220–223*, 272–288.

Neave, D. A., & Putirka, K. D. (2017). A new clinopyroxene-liquid barometer, and implications for magma storage pressures under Icelandic rift zones. *American Mineralogist 102*(4), 777–794.

Norman Levi Bowen & John Frank Schairer. (1935). The system MgO-FeO-SiO $_2$. *American Journal of Science*, *s5-29*(170), 151.

O'Neill, C., & Sigloch, K. (2018). Crust and Mantle Structure Beneath the Azores Hotspot—Evidence from Geophysics. In U. Kueppers & C. Beier (A c. Di), *Volcanoes of the Azores* (pp. 71–87). Springer Berlin Heidelberg.

Roeder, P. L., & Emslie, R. F. (1970). Olivine-liquid equilibrium. *Contributions to Mineralogy and Petrology*, *29*(4), 275–289.

Ubide, T., Neave, D. A., Petrelli, M., & Longpré, M.-A. (2021). Editorial: Crystal Archives of Magmatic Processes. *Frontiers in Earth Science*, *9*, 749100.

Viveiros, F., Silva, C., Moreno, L., Pacheco, J. E., & Ferreira, T. (s.d.). Secondary manifestations of volcanism – an open window to understand geothermal resources in the Azores archipelago. *Comunicações Geológicas*, *107*(1), 89-91.

Vogt, P. R., & Jung, W. Y. (2004). The Terceira Rift as hyper-slow, hotspot-dominated oblique spreading axis: A comparison with other slow-spreading plate boundaries. *Earth and Planetary Science Letters*, *218*(1–2), 77–90.

Zanon, V., & Viveiros, F. (2019). A multi-methodological re-evaluation of the volcanic events during the 1580 CE and 1808 eruptions at São Jorge Island (Azores Archipelago, Portugal). *Journal of Volcanology and Geothermal Research*, *373*, 51–67.